[Article] doi: 10.3866/PKU.WHXB201603094 www.whxb.pku.edu.cn

乙二醇促进制备高分散的Co/SiO_2催化剂及其催化乳酸乙酯转化为1,2-丙二醇的气相加氢活性

仇松柏 翁育靖 刘琪英 马隆龙 张 琦 王铁军*
(中国科学院可再生能源重点实验室，中国科学院广州能源研究所，广州 510640)

摘要：研究了利用乙二醇共浸渍方法制备高分散的二氧化硅负载钴催化剂，该催化剂有效地提高了乳酸乙酯的气相加氢反应活性。系统地考察了钴金属负载量、乙二醇与硝酸钴摩尔比、醇种类和焙烧温度等制备参数对四氧化三钴纳米粒子物性的影响。乙二醇与硝酸钴摩尔比和醇种类对二氧化硅负载的四氧化三钴纳米粒子大小有显著影响。与常规的浸渍方法相比较，共浸渍过程中的乙二醇增强了二价钴粒子和载体二氧化硅之间的相互作用力，从而引起金属钴分散度的提高以及四氧化三钴纳米粒子粒径从16 nm降到5 nm以下；金属钴的高分散与无定型硅酸钴的形成密切相关；同时显著地提高了乳酸乙酯的加氢活性，在反应条件下(2.5 MPa、160 °C和10% (*w*，质量分数) Co/SiO_2)乳酸乙酯的转化率从69.5%提高到98.6%，1,2-丙二醇的选择性达到98.0%。利用X射线衍射(XRD)、透射电子显微镜(TEM)、X射线光电子能谱(XPS)、N_2吸脱附实验、H_2程序升温还原(H_2-TPR)等表征手段对共浸渍制备的Co/SiO_2催化剂结构和形貌进行了表征分析。

关键词：Co/SiO_2；共浸渍；乳酸乙酯加氢；1,2-丙二醇；乙二醇
中图分类号：O643

Preparation of Highly Dispersed Co/SiO_2 Catalyst Using Ethylene Glycol and Its Application in Vapor-Phase Hydrogenolysis of Ethyl Lactate to 1,2-Propanediol

QIU Song-Bai WENG Yu-Jing LIU Qi-Ying MA Long-Long ZHANG Qi WANG Tie-Jun*
(*Key Laboratory of Renewable Energy, Guangzhou Institute of Energy Conversion, Chinese Academy of Sciences, Guangzhou 510640, P. R. China*)

Abstract: Highly dispersed Co catalysts supported on SiO_2 were prepared in the presence of ethylene glycol (EG) by co-impregnation and tested in the vapor-phase hydrogenolysis of ethyl lactate to 1,2-propanediol. The synthesis parameters of Co metal loading, ratio of EG to cobalt nitrate, type of alcohol and calcination temperature, which influenced the physical properties of the Co_3O_4 nanoparticles, were investigated through the use of X-ray diffraction (XRD). It revealed that the ratio of EG to cobalt nitrate and the type of alcohol significantly affected the particle size of Co_3O_4 supported on SiO_2. During co-impregnation with EG, the interaction between Co^{2+} and the SiO_2 support was strongly enhanced, resulting in the high dispersion of cobalt species and the decrease of Co_3O_4 particle size from 16 nm to below 5 nm; the significantly enhanced cobalt dispersion was associated with the formation of amorphous cobalt silicate. Meanwhile the conversion of ethyl lactate was greatly improved to 98.6% from 69.5%, with 98.0% selectivity of 1,2-propanediol over 10% (*w*, mass fraction) Co/SiO_2 catalysts under the given reaction conditions (2.5 MPa and 160 °C). The obtained catalysts were

Received: March 1, 2016; Revised: March 7, 2016; Published on Web: March 9, 2016.
*Corresponding author. Email: wangtj@ms.giec.ac.cn; Tel: +86-20-87057751.
The project was supported by the National High-Tech Research and Development Program of China (863) (2012AA101806) and National Natural Science Foundation of China (21306195, 51276183).
国家高技术研究发展计划项目(863) (2012AA101806)及国家自然科学基金(21306195, 51276183)资助

characterized by X-ray diffraction (XRD), transmission electron microscopy (TEM), X-ray photoelectron spectroscopy (XPS), N_2 adsorption-desorption measurements, and H_2 temperature-programmed reduction (H_2-TPR) methods.

Key Words: Co/SiO_2; Co-impregnation; Ethyl lactate hydrogenation; 1,2-Propanediol; Ethylene glycol

1 Introduction

Supported metal catalysts comprise the most important class of heterogeneous catalysts in industrial practice[1]. Therefore, the synthesis of supported catalysts with high dispersion, stability, and activity is of utmost academic and industrial importance. A great deal of preparation methods have been developed to improve catalytic activity of supported catalysts, such as ion exchange[2], ion sputtering[3], atomic layer deposition[4], chemical vapor/liquid deposition[5,6], impregnation[1,7–9] and so on. By far the most used synthesis route involves impregnation, which has been opened up by many innovative pathways for achieving highly active catalysts, including complexation-impregnation[1], surface modification[10], freeze-drying[11], adjusting pH value of impregnation solution[12], organic metal precursor[1,6], calcination atmosphere[13,14], etc. In consideration of production cost and technical feasibility in industry, co-impregnation with ethylene glycol (EG) as one simple and efficient strategy of modifying impregnation for preparing the highly active catalysts is most attractive[1,15].

Biomass-derived lactic acid has been commercially produced by fermentation of renewable resources, such as sugars, starches, and xylose. Hydrogenation of lactic acid provides a promising alternative to the bulk commodity chemical production of 1,2-propanediol (1,2-PDO) which depended on the non-renewable petroleum-based process[16]. Supported cobalt catalysts have been of great interest due to their high catalytic properties in several different catalytic processes, ranging from catalytic combustion, steam reforming, Fischer-Tropsch synthesis, hydrodesulfurization, and hydrogenation of aromatics[17]. Previous reports on the hydrogenation of lactic acid by various transition metal catalysts (Ru, Pd, Ni, Fe, Cu, and Co) have indicated that Co-based catalysts are significantly more active and selective[18,19]. However, it is acknowledged that the preparation method could show an obvious effect on the activity of lactic acid hydrogenation by adjusting the dispersion and particles size of cobalt species[16–19].

Formerly, we have prepared highly active and dispersed nickel based catalysts by co-impregnation with polyols such as EG[15,20]. Comparing with the conventional wetness impregnation, the only difference of co-impregnation needs to add moderate polyols into the metal nitrate aqueous solution before impregnation. Upon solvent evaporation, additive polyols increase viscosity of such solutions and form a gel-like film to inhibit redistribution of the active phase over the support bodies during drying, resulting in formation of smaller metal particles and high dispersions[1,7]. In this paper, highly dispersed Co catalysts supported on SiO_2 were prepared by co-impregnation with EG and tested in the vapor-phase hydrogenolysis of ethy lactate to 1,2-propanediol. The synthesis parameters that influence the physical property of Co_3O_4 nanoparticles were investigated, including Co metal loading, ratio of EG to cobalt nitrate, types of alcohol, and calcination temperature. The obtained catalysts were characterized by XRD, TEM, XPS, BET (Brunauer-Emmett-Teller), and H_2-TPR analytical methods.

2 Experimental

Co/SiO_2 catalysts with 1.0%–40.0% (*w*, mass fraction) Co loading were prepared by incipient-wetness impregnation and co-impregnation[15] on SiO_2 support (Qingdao Haiyang Chemical Co., Ltd, 60–80 mesh, specific surface area of 352.4 $m^2 \cdot g^{-1}$, pore volume of 1.07 $mL \cdot g^{-1}$, average pore diameter of 9.45 nm) with $Co(NO_3)_2 \cdot 6H_2O$ (analytical pure, 99.0%) in aqueous solution. The Co loading was the nominal metal loading, which was calculated by the equation of $(W_{Co}/W_{support}) \times 100\%$, where W_{Co} and $W_{support}$ were the masses of cobalt and SiO_2 support, respectively. Before impregnation, the SiO_2 support was calcined in air at 550 °C for 4 h. Then, the cobalt nitrate aqueous solution was impregnated onto SiO_2 support and kept still for 12 h. After that, the samples were dried at 100 °C and calcined at 400 °C for 2 h using a heating rate of 2 $°C \cdot min^{-1}$. The preparation process of co-impregnation was the same with that of the conventional wetness impregnation method except adding proper amount of EG (analytical pure, 99.6%) into the metal nitrate aqueous solution. The obtained catalysts were denoted as $Co/SiO_2 \cdot x$EG (molar ratio of *x*(Co/EG) is 1 : *x*). The sample, $Co/SiO_2 \cdot 0$EG, which prepared by conventional wetness impregnation without EG addition, was used as a reference. Ethy lactate (analytical pure, 99.0%) was supplied by Aladdin Industrial Corporation.

The BET (Brunauer-Emmett-Teller) specific surface area of catalysts was determined by N_2 isothermal adsorption using QUADRASORB SI analyzer equipped with QuadraWin software system. H_2-TPR researches of the different catalysts were carried out in a quartz tube reactor with a thermal conductivity detector (TCD) reported in literature[21]. XRD patterns were measured by an X′pert Pro Philips diffractometer, using Cu K_α radiation (λ = 0.1541841 nm) in the range of $2\theta = 5°–80°$, step counting time of 10 s, and step size of 0.0167° at 25 °C. The XPS analysis was performed on a ThermoFisher Scientific ESCALAB 250 spectrometer. The spectra were excited by the monochromatized Al K_α source (1486.6 eV). The average Co_3O_4 particle sizes were calculated from the most intense Co_3O_4 line ($2\theta = 36.8°$, (311) crystal plane), using the Scherrer formula.

The vapor-phase hydrogenolysis of ethy lactate was carried out in a tubular stainless steel fixed-bed reactor (inner diameter of 10 mm and length of 350 mm). Before reaction, 2 mL catalysts (about 1.2 g) were loaded in the constant temperature zone of the reactor

with quartz sand and quartz wool as the filler materials on the top and bottom of the reactor, respectively. Subsequently, the catalysts were *in situ* reduced in a H_2 flowing at 550 °C for 8 h at 2.5 MPa. During reaction, analytical pure ethy lactate was pumped into the fixed-bed reactor at the flow rate of 0.010 mL·min^{-1} by a high pressure liquid pump (HPLP). The reaction temperature varied from 140 to 200 °C. The gas stream at the reactor outlet was connected to a cooler that was maintained at 4 °C. The condensed samples were collected regularly and analyzed by gas chromatography (GC-2014C, Shimadzu) equipped with a flame ionization detector and a HP-Innowax capillary column (30 m × 0.25 mm × 0.25 μm).

3 Results and discussion

3.1 Catalyst characterization

The synthesis parameters such as the molar ratio of cobalt to EG nitrate, the types of alcohol, the Co metal loading, and the calcination temperature, which influenced the physical property of Co_3O_4 nanoparticles, were investigated through the use of XRD method shown in Fig.1. In the diffraction patterns of all the catalysts, the broad and diffuse pattern observed clearly at around 2θ = 22.5° was attributed to amorphous silica[17]. The samples showed diffraction lines at 31.2° (220), 36.8° (311), 44.8° (400), 59.4° (511), and 65.2° (440), indicating that cobalt was present mainly in the form of Co_3O_4 spinel structure (JCPDS No. 74-1656) after calcination at 400 °C[18]. However, there were no XRD peaks of cobalt phyllosilicate to be detected on all the Co/SiO_2 samples. The average Co_3O_4 particle sizes were calculated from the most intense Co_3O_4 line (2θ = 36.8°), using the Scherrer formula. Fig.1A showed the XRD patterns of the 10% Co/SiO_2 catalysts with different molar ratios of cobalt nitrate to EG. The samples with *x* (Co/EG) from 1 : 1 to 1 : 10 gave weak and broad peaks to Co_3O_4 below 5 nm, indicating that Co_3O_4 particles were very small and highly dispersed on the SiO_2 support. Interestingly, no diffraction lines pertaining to the Co/SiO_2 with *x*(Co/EG) ≤ 1 : 2 were observed, due to small particle sizes near or amorphous cobalt species below the limitation for the XRD detectability. While the samples with *x*(Co/EG) = 1 : 0 and 1 : 0.5 showed the strong and sharp Co_3O_4 peaks respectively corresponding to 16 and 15 nm, which means that the Co_3O_4 particles grew up. The average crystal sizes of Co_3O_4 decreased gradually from 16 nm to below 5 nm with the increasing amount of EG. It implied that the molar ratios of *x*(Co/EG) played a vital role in controlling particle sizes of Co_3O_4 and dispersion of cobalt species on the SiO_2 support.

As shown in Fig.1B, the types of alcohol significantly affected the particle size of Co_3O_4 supported on SiO_2 (10% Co loading). Other polyols such as glycerol (Gly) and citric acid (CA) have actually similar physical and chemical properties, which could play the same role in impregnation process as ethylene glycol[20]. However, upon solvent evaporation, ethanol (Eth) in the cobalt nitrate aqueous solution could volatilize completely during drying because of its lower boiling point and viscosity than other polyols, which could not inhibit redistribution of the active phase over the support bodies, resulting in formation of 16 nm Co_3O_4.

Fig.1C displayed the XRD profiles of the Co/SiO_2 samples with the different Co metal loading varying from 1%−40% with *x*(Co/

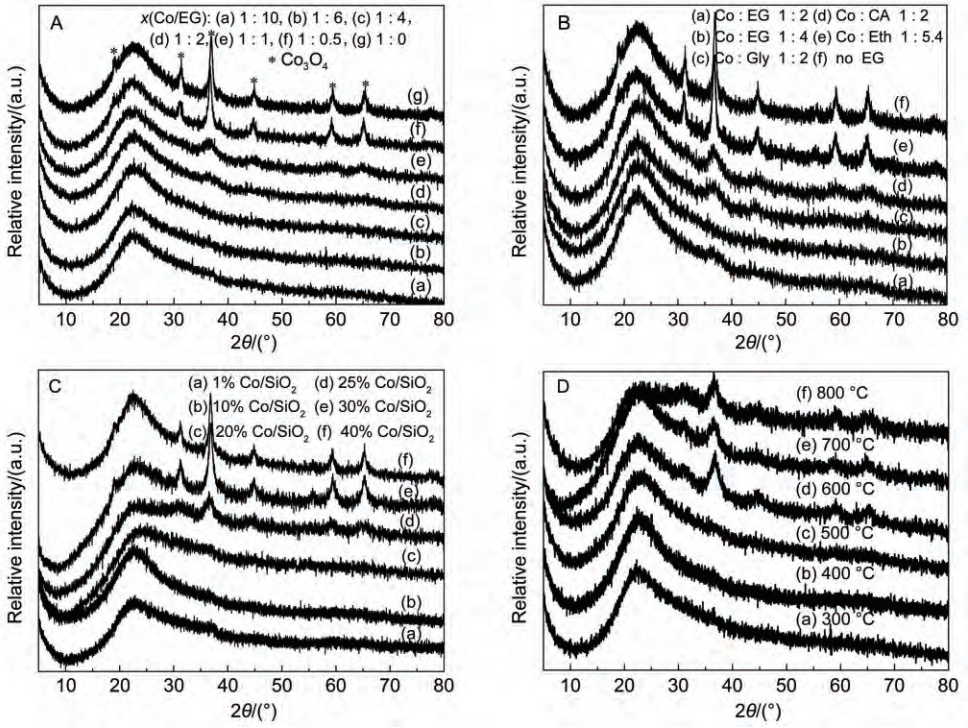

Fig.1 XRD patterns of various catalysts

(A) 10% Co/SiO_2 catalysts with different molar ratios of cobalt nitrate to EG; (B) 10% Co/SiO_2 catalysts with ethanol (Eth) and different polyols including glycerol (Gly) and citric acid (CA); the effect of (C) the Co metal loading and (D) the calcination temperature (10% Co/SiO_2) with *x*(Co/EG) = 1 : 2

EG) = 1 : 2. There are no other XRD diffraction peaks to be detected in 1%−20% Co/SiO_2 catalysts, indicating that metal oxides dispersed well on the support, and metal oxide crystallite size should be smaller than 4 nm. For the Co-based catalysts with higher metal loading over 25%, new dispersive diffraction peaks could be found and gradually got strong and sharp, indicating that the mean particle sizes of Co_3O_4 slowly grew up to 13 nm. A conclusion could be obtained that the cobalt oxidized species were considered evenly dispersed on the surface of the support and could form superfine Co_3O_4 nanoparticles below 4 nm until metal loading amount exceeded 30%. This clearly showed that additive EG during impregnation had no ability to control relatively homogeneous particle sizes and high dispersion for excess metal loading over 30%. This might be caused by the small BET specific surface area of SiO_2 support, which could not support excess metal over 30% Co loading for maintaining high metal dispersion.

Fig.1D showed the diffraction patterns of 10% Co/SiO_2 samples with x(Co/EG) = 1 : 2 calcinated at different temperatures. The calcination temperatures had a minor impact on particle size and distribution. Particularly, the diffraction peaks of Co_3O_4 completely disappeared after calcination below 600 °C, due to small particle sizes below the limitation for the XRD detectability. Even at higher calcination temperature in the range of 600−800 °C, the Co/SiO_2 samples also obviously expressed the broad and diffuse pattern of Co_3O_4 with an average diameter of about 5 nm, indicating the favorable resistance to high temperature sintering using the co-impregnation method with EG. Generally, as the calcination temperature got higher, the particles were easy to agglomerate and the particles got bigger using common impregnation method. Thus, the Co/SiO_2 catalyst prepared by co-impregnation exhibited the wide temperature window of calcination and excellent resistance to metal sintering as stronger interaction between the supported Co and silica support[22].

So as to explore the textural and physicochemical properties using co-impregnation, the Co/SiO_2 sample with x(Co/EG) = 1 : 1 was comparatively studied with the Co/SiO_2 catalyst without EG using conventional wetness impregnation. The TEM images of Co/SiO_2·0EG and Co/SiO_2·1EG were also shown in Fig.2(a, b). As could be seen, the TEM microstructures were significantly different with cobalt phyllosilicate species, which exhibited amorphous lamellar structure, constituted of claylike lines in literature[23]. The TEM photographs clearly showed that the Co/SiO_2·1EG catalyst exhibited remarkably smaller particle size. In addition, the Co_3O_4 nanoparticles were spherical and distributed homogeneously with an average diameter of about 7 nm, which was a little larger than the values calculated from the XRD data, as tabulated in Table 1. This might be caused by imaging techniques such as TEM which often gave the size of the particle, while X-ray diffraction disclosed the size of the crystalline. For the Co/SiO_2·0EG, cobalt oxide particle aggregated into even larger clusters on the SiO_2 surface with maldistribution in the range of 40−130 nm.

After impregnating, the BET special surface area and total pore volume obviously decreased. The impregnation and drying steps had not significantly affected the long-range order of the mesopores. The decreased porosity was presumably due to the formation of inaccessible domains in the sample. Moreover, the pore diameters for all samples were almost same to the original SiO_2, suggesting that cobalt species were basically limited on the external surface of the mesoporous support, which was in agreement with the XPS data shown below.

The XPS study was carried out to determine the chemical composition and valence state of the elements on the surface of supported cobalt oxide as shown in Fig.3. The signal of the Co 2*p* lines exhibited a slightly intense satellite structure. For 10% Co/SiO_2·0EG and 10% Co/SiO_2·1EG catalysts, the binding energy

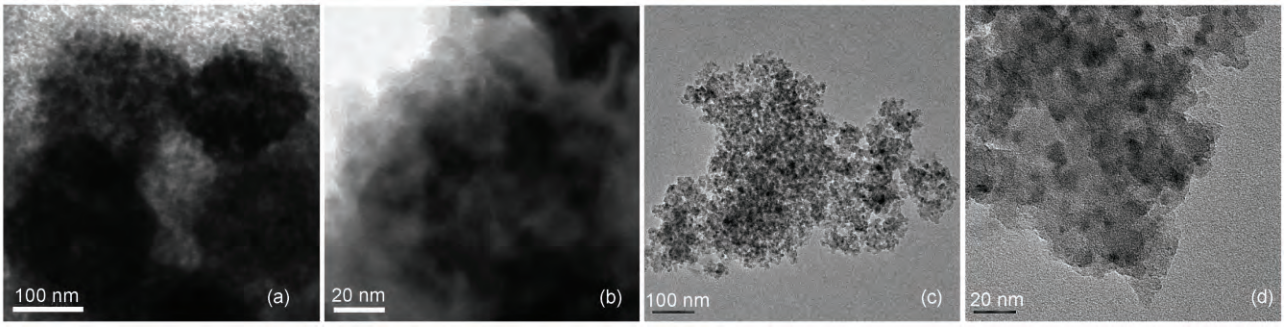

Fig.2 TEM images of 10% Co/SiO_2·0EG (a, b) and 10% Co/SiO_2·1EG (c, d)

Table 1 Textural properties of the catalysts

Catalyst	Molar ratio of Co/EG	Metal loading/%[a]	S_{BET}/($m^2 \cdot g^{-1}$)	Pore volume/($cm^3 \cdot g^{-1}$)[b]	Average pore diameter/nm	Mean particle size/nm[c]
SiO_2	–	–	352.4	1.07	9.45	–
10% Co/SiO_2·0EG	1 : 0	8.32	240.0	0.72	9.64	16 (78[d])
10% Co/SiO_2·1EG	1 : 1	8.59	270.8	0.83	9.62	5 (7[d])

[a]determined from inductively coupled plasma atomic emission spectrometry (ICP-AES). [b]Surface areas and pore volumes and diameters of the samples were calculated using standard BET and BJH theory, respectively. [c]Particle size was calculated by Scherrer's equation, the Bragg angle of 2θ using 36.8° ((311) crystal plane).
[d]Particle size was observed by TEM, distributed in the ranges of 40−130 and 13−4 nm, respectively.

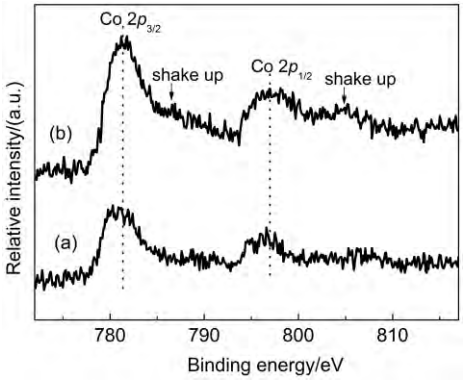

Fig.3 Co 2*p* XPS spectra of (a) 10% Co/SiO_2·0EG and (b) 10% Co/SiO_2·1EG

(BE) of the Co $2p_{3/2}$ showed peaks at 780.7 and 781.3 eV, respectively. The higher position of the Co $2p_{3/2}$ peaks indicated a stronger interaction between silica support and cobalt species[24]. For 10% Co/SiO_2·0EG, the binding energy and low intensity of shake-up satellites suggested that Co_3O_4 was the predominant cobalt phase on the catalyst surface[25,26], which was in good agreement with the other measurements obtained from XRD and H_2-TPR. In the case of the catalyst with co-impregnation, the relative intensity of the shake-up satellite obviously increased. Furthermore, the main Co $2p_{3/2}$ peak shifted to higher binding energy, with satellite peaks at about 6 eV higher energy sides. These features were indicative of the presence of Co^{2+} species in amorphous cobalt silicate and could be taken as evidence of a strong interaction of the cobalt species with the SiO_2 support[25−28], which were responsible for the H_2-TPR profiles at high temperature, as observed later. Therefore, these results suggested that both amorphous cobalt silicate and Co_3O_4 were mainly formed over the catalyst prepared by co-impregnation with EG. Generally, the decomposition of organic cobalt precursors could facilitate a strong Co-support interaction, resulting in the appearance of Co_3O_4 crystallites and amorphous cobalt silicate. Table 2 presented the atomic concentration and corresponding atomic ratio of XPS results. Based on XPS carbon analysis, the surface carbon concentration had a little increase, which revealed that the EG decomposed almost completely during calcining at 400 °C in air. The sample of 10% Co/SiO_2·0EG also expressed the carbon peak during impregnation without EG, which could be ascribed to carbon pollution. XPS intensity ratios of I_{Co}/I_{Si} could provide important information about the dispersion[29]. Compared with the conventional wetness impregnation, the co-impregnation increased the surface cobalt content and I_{Co}/I_{Si} ratios by almost 50% using the addition of EG, which meaned the higher surface dispersion. Thus, cobalt dispersion in the calcinated cobalt catalysts was significantly affected by the EG in the impregnating solution.

On the other hand, in order to further explore the effect of additive EG on the dispersion of cobalt species in the Co/SiO_2 samples, the H_2-TPR technique was measured as shown in Fig.4. In the reduction profile of calcined 10% Co/SiO_2·0EG, two main peaks were evolved at around 366 and 450 °C (Fig.4(a)), which were ascribed to reduction of Co_3O_4 to CoO (366 °C) and CoO to Co^0 (450 °C), respectively, according to the literature[18,30]. As observed, the small peak at 760 °C could be attributed to the cobalt

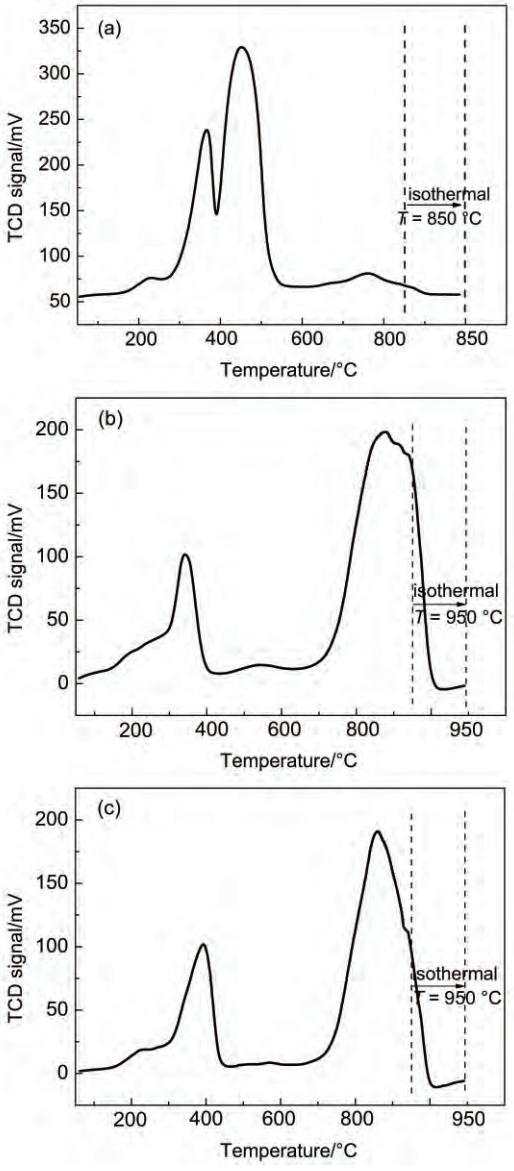

Fig.4 H_2-TPR of Co/SiO_2 samples

(a) 10% Co/SiO_2·0EG and (b) 10% Co/SiO_2·1EG after calcinating at 400 °C for 2 h; (c) 10% Co/SiO_2·1EG after calcinating at 550 °C for 4 h

Table 2 XPS results for 10% Co/SiO_2 catalysts

Catalyst	Molar ratio Co/EG	BE(Co $2p_{3/2}$)/eV	Atomic concentration/%				Atomic ratio/%	
			Co	Si	C	O	Co/Si	C/Si
10% Co/SiO_2·0EG	1 : 0	780.7	0.94	23.67	2.76	72.63	3.97	11.66
10% Co/SiO_2·1EG	1 : 1	781.3	1.37	23.30	3.13	72.20	5.88	13.43

species interacting strongly with silica[23]. In the previous study, TPR peak above 700 °C was assigned to the reduction of Co silicate, probably formed by reaction of Co^{2+} species strongly interacting with the SiO_2 support. On the other hand, a significantly different reduction pattern was observed for the samples obtained by co-impregnation using EG[30]. One small asymmetric peak shifted to the lower temperature around 340 °C, typical of Co_3O_4 reduction with small nanoparticles, ascribing to the weak interaction with support. Meanwhile, the main reduction feature for this sample was detected at higher temperature of about 870 °C, relating to the reduction of amorphous Co_2SiO_4, which was consistent with XPS results. In order to eliminate the influences of the residual carbon species to the reduction profile at high temperature, 10% Co/SiO_2·1EG was calcinated at 550 °C for 4 h as a reference. The samples calcinated at higher temperature expressed the similar H_2-TPR profiles. Generally the strong interaction between the metal species and support favored to enhance Co dispersion and form ultra-small particles. Taking into consideration of XRD, TEM, XPS, and TPR analyses, two main kinds of cobalt species (small size of Co_3O_4 nanoparticles and amorphous Co_2SiO_4) were inferred to present in the samples prepared by co-impregnation using EG, corresponding to weak and strong interaction between cobalt particles and SiO_2 support, respectively. The strong interaction was mainly caused by the existence of amorphous cobalt silicate.

3.2 Catalytic performance

So as to explore the catalytic activity using co-impregnation, the Co/SiO_2 samples with *x*(Co/EG) = 1 : 1 was compared with the catalyst by conventional wetness impregnation in the ethyl lactate hydrogenation. As illustrated in Fig.5, the desired product 1,2-PDO was formed mainly *via* the direct hydrogenation of ethyl lactate over the Co/SiO_2 catalysts. The chief by-products included 1-pronanol (1-PO), 2-propanol (2-PO), lactic acid, and 2-hydroxyl propyl lactate. The hydrogenolysis reaction was performed in the fixed-bed reactor with the typical reaction conditions at 2.5 MPa, weight hourly space velocity (WHSV) of 0.3 h^{-1}, and H_2/ethy lactate molar ratio of 100 : 1. Table 3 presented the effect of cobalt loading and reaction temperature on the reaction performance. The conversion of ethyl lactate increased with the increasing cobalt loading, and the 1,2-propanediol selectivity decreased slightly. The

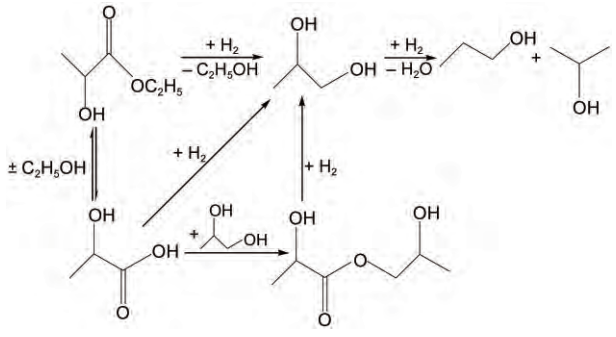

Fig.5 Possible reaction scheme for the hydrogenation of ethyl lactate

Co/SiO_2 catalysts showed almost complete conversion with cobalt loading above 15% at 160 °C. The conversion and selectivity for ethyl lactate hydrogenolysis was investigated on the Co/SiO_2 samples at 140, 160, and 200 °C. As expected, the conversion of ethyl lactate increased remarkably as the reaction temperature elevated from 140 to 160 °C. This could be caused by the low boiling point of ethyl lactate (154 °C), resulting in the different hydrogenolysis state of reactant such as vapor-phase and liquid-phase. The selectivity of 1,2-PDO dramatically decreased at a temperature of 200 °C, especially for the highly active 10% Co/SiO_2·1EG. The decrease of 1,2-PDO selectivity was mainly due to dehydration that produced 1-pronanol (1-PO) and 2-propanol (2-PO), indicating that overhigh reaction temperature favored the formation of side products.

In comparison with the catalysts prepared by conventional wetness impregnation, the Co/SiO_2 *via* co-impregnation with EG presented markedly higher catalytic activity in the ethyl lactate hydrogenation. Especially, the conversion of ethyl lactate was greatly enhanced from 69.5% to 98.6% at 160 °C over 10% Co/SiO_2. Even at low cobalt loading of 5% Co/SiO_2·1EG, there was 55.5% ethyl lactate conversion. Thus, the catalytic activity of Co/SiO_2 catalysts could be strongly enhanced by co-impregnation, apparently related to the ultra-small particles and higher dispersion originated from the strong interaction between cobalt particles and SiO_2 support. The long-term stability and activity of 10% Co/SiO_2·1EG catalyst were tested for vapor-phase hydrogenation of ethy lactate. Obvious decrease of ethy lactate conversion was observed within 50 h under identical reaction conditions.

In brief, the catalytic activity was dependent on the number of active cobalt species[29]. It was proved that the reaction activity was directly correlated with the cobalt dispersion of the supported

Table 3 Activity of various catalysts under different reaction temperatures[a]

Catalyst	Reaction temperature/°C	Ethy lactate conversion/%	Selectivity[b]/%			
			1,2-PDO	1-PO	2-PO	others[c]
7% Co/SiO_2·0EG	160	43.6	98.7	1.0	0	0.3
10% Co/SiO_2·0EG	140	29.4	97.8	1.1	0.5	0.7
10% Co/SiO_2·0EG	160	69.5	98.2	0.7	0.2	0.9
10% Co/SiO_2·0EG	200	85.6	84.6	7.5	5.3	2.6
15% Co/SiO_2·0EG	160	99.9	95.0	3.3	1.2	0.5
25% Co/SiO_2·0EG	160	99.0	95.5	2.4	0.8	1.3
5% Co/SiO_2·1EG	160	55.5	99.1	0.3	0.2	0.4
7% Co/SiO_2·1EG	160	66.3	97.3	1.4	0.3	1.0
10% Co/SiO_2·1EG	140	49.6	99.1	0.6	0.1	0.2
10% Co/SiO_2·1EG	160	98.6	98.0	1.0	0.4	0.6
10% Co/SiO_2·1EG	200	98.9	58.3	26.7	13.2	1.8
15% Co/SiO_2·1EG	160	98.0	97.4	1.5	0.5	0.6
25% Co/SiO_2·1EG	160	97.6	97.6	1.2	0.4	0.8
[d]10% Co/SiO_2·1EG	160	90.2	97.4	1.0	0.5	1.1

[a]reaction conditions: 140−200 °C, 2.5 MPa, WHSV = 0.3 h^{-1} and H_2/ethy lactate = 100 : 1 (molar ratio). [b]1,2-PDO, 1-PO, 2-PO standed for 1,2-propanediol, 1-pronanol, and 2-propanol, respectively. [c]Other products mainly included lactic acid and 2-hydroxyl propyl lactate. [d]The liquid products within 45−50 h were collected and tested for evaluating the stability.

metal catalysts in the Fishcher-Tropsch reactions and citral hydrogenation. The XRD and TEM obviously showed that the additive EG during co-impregnation inhibited aggregation of the active phase over the support surface resulting in formation of smaller metal particles and significantly improved the dispersion of supported cobalt.

As observed analysis techniques, a strong interaction between SiO_2 support and cobalt oxide species indicated an electron transfer from cobalt oxide to support for the Co/SiO_2 samples prepared by co-impregnation, contributing to low electron density of Co^{2+} species in amorphous Co_2SiO_4; furthermore, the weak interaction was inferred to the electron density of supported Co ions, expressing in ultra-small Co_3O_4 nanoparticles. The co-impregnation increased the surface cobalt content and I_{Co}/I_{Si} ratios by 48.1%, which was an interesting coincidence with the activity improvement of ethyl lactate conversion with 41.9% increasement at 160 °C over 10% Co/SiO_2, indicating that the excellent hydrogenation activity was mainly caused by the high dispersion of Co active sites. The hydrogenation of ethyl lactate required both of the dissociation of hydrogen and activation of C=O bond[16]. XPS and TPR results demonstrated that weak and strong interaction occurred between cobalt species and SiO_2 support, making difference of Co electron density. It was reported that higher electron density on Co active sites could facilitate the formation of activated hydrogen, which was corresponded to the cobalt species with the weak interaction[16,31]. The lower electron density of the cobalt species with the strong interaction might be beneficial to the activation of C=O bond[16]. Thus, the excellent performance of 10% Co/SiO_2·1EG catalyst was mainly attributed to the weak interaction cobalt species and SiO_2 support, its surface composition with high I_{Co}/I_{Si} ratios, and relatively high dispersion of particles and Co active sites.

4 Conclusions

The Co/SiO_2 catalysts prepared by co-impregnation with EG showed excellent activity in the vapor-phase hydrogenolysis of ethyl lactate to 1,2-propanediol. The synthesis parameters such as the Co loading, the molar ratio of cobalt to EG, the types of alcohol additives, and the calcination temperature were carefully studied. Where, the molar ratios of cobalt to EG, and the types of alcohol additives played critical roles in controlling particle sizes and dispersion of Co_3O_4 on the SiO_2 support. Under the promotion of EG with higher boiling point and viscosity, the average crystal sizes of supported Co_3O_4 decreased from 16 nm to below 5 nm with the molar ratio of cobalt to EG above 1 : 1. For excess metal loading over 30%, additive EG during impregnation had no ability to control relatively homogeneous particle sizes and high dispersion. The strong interaction between the Co species and the silica support led to the wide temperature range of calcination and excellent resistance to supported metal sintering even at 800 °C. In comparison with the catalysts prepared by conventional wetness impregnation, the conversion of ethy lactate was greatly enhanced to 98.6% from 69.5%, with 98.0% selectivity of 1,2-propanediol over 10% Co/SiO_2 catalysts *via* co-impregnation at 2.5 MPa and 160 °C. As observed from XPS and TPR techniques, two main kinds of cobalt species (Co_3O_4 with super small particle size and amorphous Co_2SiO_4) were inferred to present in the samples prepared by co-impregnation using EG, corresponding to weak and strong interaction between cobalt species and SiO_2 support, respectively. The excellent performance of 10% Co/SiO_2·1EG catalyst could be mainly attributed to the weak interaction cobalt species and SiO_2 support, its surface composition with high I_{Co}/I_{Si} ratios, and relatively high dispersion of particles and Co active sites.

References

(1) Dillen, A. J.; Terörde, R. M.; Lensveld, D. J.; Geus, J. W.; Jong, K. P. *J. Catal.* **2003,** *216*, 257. doi: 10.1016/S0021-9517(02)00130-6

(2) Centomo, P.; Bonato, I.; Hankova, L.; Holub, L.; Jerabek, K.; Zecca, M. *Top. Catal.* **2013,** *56* (9−10), 611. doi: 10.1007/s11244-013-0021-6

(3) Zeng, C. Y. ; Sun, J.; Yang, G. H.; Ooki, I.; Hayashi, K.; Yoneyama, Y.; Taguchi, A.; Abe, T.; Tsubaki, N. *Fuel* **2013,** *112*, 140. doi: 10.1016/j.fuel.2013.05.026

(4) Detavernier, C.; Dendooven, J.; Sree, S. P.; Ludwig, K. F.; Martens, J. A. *Chem. Soc. Rev.* **2011,** *40* (11), 5242. doi: 10.1039/c1cs15091j

(5) Liu, X. H.; Tang, D. S.; Zeng, C. L.; Hai, K.; Xie, S. S. *Acta Phys. -Chim. Sin.* **2007,** *23* (3), 361. [刘星辉, 唐东升, 曾春来, 海 阔, 解思深. 物理化学学报, **2007,** *23* (3), 361.] doi: 10.1016/S1872-1508(07)60027-8

(6) Maki-Arvela, P.; Murzin, D. Y. *Appl. Catal. A-Gen.* **2013,** *451*, 251. doi: 10.1016/j.apcata.2012.10.012

(7) Tan, X. H.; Zhou, G. B.; Dou, R. F.; Pei, Y.; Fan, K. N.; Qiao, M. H., Sun, B.; Zong, B. N. *Acta Phys. -Chim. Sin.* **2014,** *30* (5), 932. [谭晓荷, 周功兵, 窦镕飞, 裴 燕, 范康年, 乔明华, 孙斌, 宗保宁. 物理化学学报, **2014,** *30* (5), 932.] doi: 10.3866/PKU.WHXB201403212

(8) Yuan, L. X.; Chen, Y. Q.; Song, C. F.; Ye, T. Q.; Guo, Q. X.; Zhu, Q. S.; Torimoto, Y.; Li, Q. X. *Chem. Commun.* **2008,** *41*, 5215. doi: 10.1039/B810851J

(9) Guo, J. H.; Ruan, R. X.; Zhang, Y. *Ind. Eng. Chem. Res.* **2012,** *51* (19), 6599. doi: 10.1021/ie300106r

(10) Qu, Z. P.; Huang, W. X.; Zhou, S. T.; Zheng, H.; Liu, X. M.; Cheng, M. J.; Bao, X. H. *J. Catal.* **2005,** *234*, 33. doi: 10.1016/j.jcat.2005.05.021

(11) Eggenhuisen, T. M.; Munnik, P.; Talsma, H.; de Jongh, P. E.; de Jong, K. P. *J. Catal.* **2013,** *297*, 306. doi: 10.1016/j.jcat.2012.10.024

(12) Zhu, X. R.; Cho, H. R.; Pasupong, M.; Regalbuto, J. R. *Catalysis* **2013,** *3* (4), 625. doi: 10.1021/cs3008347

(13) Jia, L. T.; Fang, K. G.; Chen, J. G.; Sun, Y. H. *Acta Phys. -Chim. Sin.* **2006,** *22* (11), 1404. [贾丽涛, 房克功,

陈建刚, 孙予罕. 物理化学学报, **2006,** *22* (11), 1404.] doi: 10.3866/PKU.WHXB20061119

(14) den Breejen, J. P.; Sietsma, J. R. A.; Friedrich, H.; Bitter, J. H.; de Jong, K. P. *J. Catal.* **2010,** *270* (1), 146. doi: 10.1016/j.jcat.2009.12.015

(15) Qiu, S. B.; Zhang, X.; Liu, Q. Y.; Wang, T. J.; Zhang, Q.; Ma, L. L. *Catal. Commun.* **2013,** *42*, 73. doi: 10.1016/j.catcom.2013.07.031

(16) Ma, X. Y.; De, S.; Zhao, F. W.; Du, C. H. *Catal. Commun.* **2015,** *60*, 124. doi: 10.1016/j.catcom.2014.11.027

(17) Zhang, Q. H.; Chen, C.; Wang, M.; Cai, J. Y.; Xu, J.; Xia, C. G. *Nanoscale Res. Lett.* **2011,** *6*, 586. doi: 10.1186/1556-276X-6-586

(18) Huang, L.; Zhu, Y. L.; Zheng, H. Y.; Du, M. X.; Li, Y. W. *Appl. Catal. A-Gen.* **2008,** *349* (1−2), 204. doi: 10.1016/j.apcata.2008.07.031

(19) Kasinathan, P.; Yoon, J. W.; Hwang, D. W.; Lee, U. H.; Hwang, J. S.; Hwang, Y. K.; Chang, J. S. *Appl. Catal. A-Gen.* **2013,** *451*, 236. doi: 10.1016/j.apcata.2012.10.027

(20) Qiu, S. B.; Weng, Y. J.; Li, Y. P.; Ma, L. L.; Zhang, Q.; Wang, T. J. *Chin. J. Chem. Phys.* **2014,** *27* (4), 433. 10.1063/1674-0068/27/04/433-438

(21) Liu, Q. Y.; Bie, Y. W.; Qiu, S. B.; Zhang, Q.; Sainio, J.; Wang, T. J.; Ma, L. L.; Lehtonen, J. *Appl. Catal. B-Environ.* **2014,** *147*, 236. doi: 10.1016/j.apcatb.2013.08.045

(22) Lv, X. Y.; Chen, J. F.; Tan, Y. S.; Zhang, Y. *Catal. Commun.* **2012,** *20*, 6. doi: 10.1016/j.catcom.2012.01.002

(23) Xue, J. J.; Cui, F.; Huang, Z. W.; Zuo, J. L.; Chen, J.; Xia, C. G. *Chin. J. Catal.* **2012,** *33*, 1642. [薛晶晶, 崔　芳, 黄志威, 左建良, 陈　静, 夏春谷. 催化学报, **2012,** *33*, 1642.] doi: 10.1016/S1872-2067(11)60434-8

(24) Martinez, A.; Lopez, C.; Marquez, F.; Diaz, I. *J. Catal.* **2003,** *220*, 486. doi: 10.1016/S0021-9517(03)00289-6

(25) Ernst, B.; Libs, S .; Chaumette, P.; Kiennemann, A. *Appl. Catal. A-Gen.* **1999,** *186*, 145. doi: 10.1016/S0926-860X(99)00170-2

(26) Koizumi, N.; Mochizuki, T.; Yamada, M. *Catal. Today* **2009,** *141*, 34. doi: 10.1016/j.cattod.2008.03.020

(27) Mochizuki, T.; Hara, T.; Koizumi, N.; Yamada, M. *Appl. Catal. A-Gen.* **2007,** *317*, 97. doi: 10.1016/j.apcata.2006.10.005

(28) Grams, J.; Ura, A.; Kwapinski, W. *Fuel* **2014,** *122*, 301. doi: 10.1016/j.fuel.2014.01.005

(29) Girardon, J. S.; Quinet, E.; Griboval-Constant, A.; Chernavskii, P. A.; Gengembre, L.; Khodakov, A. Y. *J. Catal.* **2007,** *248*, 143. doi: 10.1016/j.jcat.2007.03.002

(30) Koizumi, N.; Suzuki, S.; Niiyama, S.; Shindo, T.; Yamada, M. *Catal. Lett.* **2011,** *141*, 931. doi: 10.1007/s10562-011-0633-z

(31) Noller, H.; Lin, W. M. *J. Catal.* **1984,** *85*, 25. doi: 10.1016/0021-9517(84)90106-4